

# Understanding What Vision-Language Models See in Traffic: PixelSHAP for Object-Level Attribution in Autonomous Driving

Anonymous ICCV 2025 DriveX submission

Paper ID XXXX

## Abstract

**001** Vision-Language Models (VLMs) are increasingly used in  
**002** autonomous driving for scene understanding, hazard de-  
**003** tection, and decision-making support. Yet, knowing which  
**004** traffic objects these models prioritize is crucial for safety  
**005** validation and trust. Existing interpretability methods pro-  
**006** vide pixel-level attributions but fail to answer the key ques-  
**007** tion: “Which specific objects—vehicles, pedestrians, traffic  
**008** signs—influence the model’s driving decisions?”

**009** We introduce **PixelSHAP**, a model-agnostic framework  
**010** for object-level explainability in Vision-Language Models  
**011** applied to traffic scenarios. PixelSHAP extends Shapley-  
**012** based attribution to structured visual entities, systemati-  
**013** cally quantifying how individual traffic participants influ-  
**014** ence a VLM’s reasoning about driving situations. Operat-  
**015** ing purely on input-output behavior, our method is compati-  
**016** ble with both open-source models (LLaVA, LLaMA-Vision)  
**017** and commercial systems (GPT-4V, Gemini) commonly used  
**018** in autonomous driving applications.

**019** Our approach introduces novel masking strategies in-  
**020** cluding Bounding Box with Overlap Avoidance (BBOA) that  
**021** address fundamental challenges in traffic scene attribution,  
**022** achieving complete object occlusion while minimizing in-  
**023** terference with neighboring vehicles or infrastructure. We  
**024** evaluate PixelSHAP on traffic scene understanding tasks,  
**025** demonstrating its ability to reveal which objects VLMs pri-  
**026** oritize for different driving scenarios. Compared to simple  
**027** baselines, PixelSHAP provides semantically meaningful at-  
**028** tributions that align with human expectations about traffic  
**029** safety priorities.

**030** Beyond technical contribution, PixelSHAP enables  
**031** safety engineers to audit VLM behavior in autonomous  
**032** driving contexts, identify potential failure modes, and vali-  
**033** date that models focus on safety-critical objects. Our imple-  
**034** mentation provides immediate practical value for develop-  
**035** ing more transparent and trustworthy autonomous driving  
**036** systems.

## 1. Introduction

037

Vision-Language Models (VLMs) are increasingly integral to autonomous driving systems, supporting scene understanding, hazard detection, and driving decision assistance. As these models move from prototypes to safety-critical deployments, understanding their decision-making is crucial for ensuring passenger safety and public trust.

Consider a scenario: a VLM analyzes a busy intersection and outputs: “Pedestrian visible in crosswalk, vehicle should yield.” This triggers braking protocols. Yet, among multiple pedestrians—on sidewalks, near the crosswalk, and one crossing—which person influenced the decision? Attribution is essential to validate that the system responded to the correct participant.



Figure 1. PixelSHAP reveals object-level attribution in traffic scenes. It identifies which pedestrian influenced the VLM’s safety assessment, enabling validation that the model focused on the actual crossing pedestrian.

The core challenge is the semantic gap between how VLMs process visual information and how we interpret their decisions for safety validation. Existing methods fall short: gradient-based approaches like GradCAM require model internals unavailable in commercial VLMs, while pixel-level perturbation methods such as RISE blur distinct traffic participants into indecipherable importance regions.

We propose PixelSHAP, a model-agnostic framework for object-level interpretability in traffic scenarios. Extending Shapley value attribution from tokens to structured visual entities, PixelSHAP quantifies how vehicles, pedestrians, traffic signs, and infrastructure influence VLM assessments.

038

039

040

041

042

043

044

045

046

047

048

049

050

051

052

053

054

055

056

057

058

059

060

061

062

063 A key innovation is our object-level perturbation approach. Our Bounding Box with Overlap Avoidance  
 064 (BBOA) achieves complete object occlusion while preserving  
 065 context for neighboring elements, enabling clean attribution  
 066 critical for safety validation.  
 067

068 This paper makes four contributions to interpretable AI  
 069 for autonomous driving:

- **Traffic-Focused Object-Level Attribution:** A framework identifying traffic participants influencing VLM decisions, compatible with open-source and commercial models.
- **BBOA Masking Strategy:** A perturbation method that occludes target objects while preserving surrounding context.
- **Multi-Model Validation:** Evaluation across four VLMs, comparing against adapted interpretability baselines.
- **Traffic Scene Evaluation:** Protocols for assessing attribution quality in driving-relevant contexts.

082 The remainder of this paper describes our methodology,  
 083 experimental validation, and implications for interpretable  
 084 autonomous driving systems.

## 085 2. Related Work

086 Understanding VLM decisions in traffic scenarios requires  
 087 explainability methods that can identify which specific vi-  
 088 sual objects influence model outputs. The choice of explain-  
 089 ability approach is fundamentally constrained by model ac-  
 090 cessibility and the semantic granularity required for safety  
 091 validation in autonomous driving applications.

### 092 2.1. White-Box vs. Black-Box Explainability

093 Explainability methods for VLMs divide into white-box ap-  
 094 proaches requiring access to model internals and black-box  
 095 methods operating solely on input-output behavior. White-  
 096 box methods like Grad-CAM [14] analyze internal gradi-  
 097 ents and activations to generate attribution maps. LVLM-  
 098 Interpret [16] provides attention visualization, relevancy  
 099 maps, and causal interpretation for vision-language models  
 100 by accessing transformer weights and gradients.

101 White-box methods offer detailed insights into model  
 102 mechanisms but face limitations for practical autonomous  
 103 driving applications. Many state-of-the-art VLMs de-  
 104 ployed in commercial autonomous systems, including GPT-  
 105 4V [7] and Gemini-2.0 [1], do not provide access to inter-  
 106 nal weights or gradients. For applications requiring inter-  
 107 pretability of production-deployed models, black-box ap-  
 108 proaches become essential.

### 109 2.2. Black-Box Perturbation-Based Methods

110 Black-box methods explain model decisions through sys-  
 111 tematic input perturbation and output analysis, making

them compatible with any VLM regardless of architec-  
 112 ture. RISE [10] generates importance maps by randomly  
 113 masking image regions and measuring output changes.  
 114 LIME [13] learns local linear approximations around input  
 115 instances using perturbation-based sampling.

116 These pixel-level approaches face limitations when ana-  
 117 lyzing traffic scenes with multiple objects. When vehicles,  
 118 pedestrians, and infrastructure appear in proximity, pixel-  
 119 based attribution creates blended importance maps that can-  
 120 not isolate individual traffic participants. For autonomous  
 121 driving safety validation, understanding which specific ob-  
 122 ject influenced a model’s assessment requires object-level  
 123 granularity that pixel-based methods cannot provide.

## 125 2.3. Shapley Values for Principled Attribution

126 Shapley values from cooperative game theory [15] provide  
 127 mathematically principled feature attribution with desirable  
 128 properties including efficiency, symmetry, and additivity.  
 129 TokenSHAP [3] demonstrated their effectiveness for lan-  
 130 guage model interpretability by quantifying individual to-  
 131 ken contributions. MM-SHAP [8] applied Shapley values  
 132 to multimodal models, measuring the relative importance  
 133 of visual versus textual modalities using image patches.

134 While Shapley-based approaches offer theoretical rigor,  
 135 existing applications focus on different granularities and  
 136 questions than object-level attribution in traffic scenarios.  
 137 Extending Shapley principles to semantic object-level anal-  
 138 ysis while maintaining black-box compatibility remains an  
 139 active area of development.

## 140 2.4. Multimodal Interpretability: Related Ap- 141 proaches and Distinctions

142 Recent interpretability frameworks for VLMs address com-  
 143 plementary aspects of multimodal understanding, though  
 144 with different focus areas than object-level attribution:

145 **MM-SHAP** [8] provides valuable insights into  
 146 modality-level contributions, quantifying whether models  
 147 rely more on textual or visual information. However, its  
 148 patch-based granularity cannot isolate individual traffic  
 149 participants within scenes. While MM-SHAP can reveal  
 150 that a model used “60% vision, 40% text,” it cannot  
 151 distinguish which specific vehicle or pedestrian drove that  
 152 visual contribution—a distinction critical for autonomous  
 153 driving safety validation.

154 **LVLM-Interpret** [16] offers comprehensive analysis  
 155 through attention visualization and causal interpretation,  
 156 providing detailed insights into model reasoning processes.  
 157 However, its dependency on white-box access to attention  
 158 weights and gradients limits applicability to commercial  
 159 VLMs commonly deployed in autonomous systems. Ad-  
 160 ditionally, its patch-based visualizations operate at spatial  
 161 resolutions that may not align with semantic object bound-  
 162aries essential for traffic safety analysis.

163 These methods address important questions about multi-  
 164 modal reasoning and provide valuable debugging capabili-  
 165 ties. Our work complements these approaches by focusing  
 166 specifically on the object-level attribution question that ex-  
 167 isting methods cannot directly address due to granularity  
 168 and accessibility constraints.

## 169 2.5. Object-Level Attribution: Addressing the 170 Granularity Gap

171 Current black-box methods cannot directly answer ques-  
 172 tions critical for traffic scene understanding: “Which spe-  
 173 cific vehicle influenced the model’s safety assessment?” or  
 174 “Did the model focus on the crossing pedestrian or back-  
 175 ground elements?” This limitation stems from the granular-  
 176 ity mismatch between available attribution methods (pixels  
 177 or patches) and the semantic units relevant for autonomous  
 178 driving validation (objects representing traffic participants).

179 The autonomous driving context amplifies these chal-  
 180 lenges because safety validation requires understand-  
 181 ing attribution at the semantic level of traffic partici-  
 182 pants—vehicles, pedestrians, cyclists, and infrastruc-  
 183 ture—rather than abstract visual regions. Existing pixel-  
 184 level methods cannot distinguish between a pedestrian ac-  
 185 tively crossing versus one standing on a sidewalk when both  
 186 appear in the same image region, yet this distinction is crit-  
 187 ical for validating autonomous driving decisions.

## 188 2.6. Our Approach

189 We introduce PixelSHAP to address the object-level attri-  
 190 bution gap by extending Shapley-based attribution to indi-  
 191 vidual traffic objects while maintaining black-box compati-  
 192 bility with commercial VLMs. Our approach builds on the  
 193 theoretical foundation of Shapley values while adapting the  
 194 methodology to operate on semantic objects rather than pix-  
 195 els or patches.

196 PixelSHAP complements existing interpretability meth-  
 197 ods by focusing on the specific granularity and accessibil-  
 198 ity requirements of autonomous driving applications. We  
 199 demonstrate improvements over adapted versions of existing  
 200 methods (RISE-Objects) and simple heuristics, showing  
 201 that principled Shapley attribution can provide more accu-  
 202 rate object-level explanations for traffic safety validation.  
 203 Our evaluation includes comparison with gradient-based  
 204 methods where applicable, providing insight into the rela-  
 205 tive performance of black-box versus white-box approaches  
 206 for object-level attribution tasks.

## 207 3. Problem Statement

208 We formalize object-level attribution in Vision-Language  
 209 Models (VLMs) as a black-box interpretability challenge:  
 210 quantifying how individual visual objects contribute to a  
 211 model’s textual output.

## 212 3.1. Problem Formulation

Given a VLM  $f$  mapping an image  $I$  and optional text prompt  $p$  to a response  $y = f(I, p)$ , our goal is to assign an attribution score  $\phi_i$  to each object  $o_i$  in  $O = \{o_1, o_2, \dots, o_n\}$ , representing its influence on  $y$ . Attribution scores must satisfy:

1. **Efficiency:**  $\sum_{i=1}^n \phi_i = f(I, p) - f(\emptyset, p)$ , where  $\emptyset$  is the scene with all objects removed. 218
2. **Symmetry:** Identical contributors receive equal scores. 219
3. **Additivity:** Scores combine consistently across object subsets. 220

## 223 3.2. Key Constraints and Requirements

**Black-Box Compatibility:** The method must function without access to model internals, gradients, or attention weights, ensuring compatibility with commercial VLMs.

**Object-Level Granularity:** Beyond pixel-level maps, we require semantic object attribution to answer, e.g., “Which specific vehicle influenced the decision?”

**Semantic Preservation:** Perturbations must fully remove an object’s contribution while maintaining scene context. 227

## 232 3.3. Applications and Use Cases

This formulation supports critical interpretability needs: In *autonomous systems*, identifying which traffic participants (vehicles, pedestrians, signs) influenced a VLM’s assessment validates correct prioritization of safety-critical objects. In *content moderation*, it clarifies which visual elements trigger policy violations, improving automated systems. In *medical imaging*, object-level attribution aids in validating diagnostic outputs and building clinician trust. In *general scene understanding*, it verifies that VLMs attend to relevant elements rather than spurious correlations. 233

## 236 3.4. Technical Challenges

**Object Segmentation Dependency:** Reliable attribution depends on accurate detection and segmentation of objects. 244

**Occlusion Strategy:** Removing an object cleanly while preserving scene context requires sophisticated masking to avoid artifacts or distortion of neighboring elements. 245

**Computational Efficiency:** Exact Shapley value computation is infeasible; efficient approximations are essential. 246

**Evaluation Methodology:** Assessing attribution quality requires ground truth aligned with human judgments of object importance. 247

The following sections describe how PixelSHAP addresses these challenges. 248

## 256 4. Methodology

PixelSHAP extends Shapley value attribution from textual tokens to visual objects, enabling principled object-level interpretability for Vision-Language Models. Our approach 257

260 operates through three stages: object identification with  
 261 segmentation, systematic perturbation, and attribution com-  
 262 putation.

#### 263 4.1. Framework Design

264 The framework requires both object detection (bounding  
 265 boxes) and segmentation masks for each object. Users  
 266 can integrate results from any detection system suited to  
 267 their application domain, including category-specific mod-  
 268 els like YOLO [11] variants or open-vocabulary systems  
 269 like GroundingDINO [6]. When detection systems provide  
 270 only bounding boxes, we automatically generate segmenta-  
 271 tion masks using SAM2 [4] within the detected regions to  
 272 ensure complete object-level analysis.

273 We formulate object attribution as a cooperative game  
 274 where detected objects serve as players and the VLM’s  
 275 response represents the outcome. For objects  $O =$   
 276  $\{o_1, o_2, \dots, o_n\}$ , each object’s Shapley value  $\phi_i$  quantifies  
 277 its contribution:

$$\phi_i = \sum_{S \subseteq O \setminus \{o_i\}} \frac{|S|!(|O| - |S| - 1)!}{|O|!} [v(S \cup \{o_i\}) - v(S)]$$

278 where  $v(S)$  measures the VLM’s response when only  
 279 objects in subset  $S$  remain visible.

#### 280 4.2. Object Perturbation Strategy

281 The central challenge lies in removing target objects while  
 282 preserving scene context for accurate attribution. We pro-  
 283 pose Bounding Box with Overlap Avoidance (BBOA) and  
 284 evaluate it against two established baselines.

285 Precise masking applies exact segmentation boundaries  
 286 but creates irregular occlusions that may introduce visual  
 287 artifacts. Bounding box masking uses rectangular regions  
 288 but risks occluding adjacent objects in dense scenes.

289 BBOA combines the advantages of both approaches  
 290 through a three-step process: first masking the target ob-  
 291 ject’s bounding box region, then identifying other objects  
 292 whose segmentation masks intersect this region, and finally  
 293 restoring those overlapping objects by unmasking their pre-  
 294 cise boundaries. This strategy ensures complete target re-  
 295 moval while preserving neighboring objects regardless of  
 296 scene density.

#### 297 4.3. Computational Implementation

298 Exact Shapley computation requires evaluating  $2^n$  object  
 299 subsets, which becomes computationally prohibitive for  
 300 scenes with many objects. We employ sampling-based ap-  
 301 proximation that reduces VLM queries from exponential to  
 302 linear scaling, typically requiring 100-300 evaluations for  
 303 scenes with 10-15 objects and completing analysis within  
 304 30-60 seconds.

305 Response similarity is measured using semantic embed-  
 306 ding approaches through sentence transformers [12] or lex-  
 307 ical similarity metrics depending on application require-  
 308 ments. The framework operates entirely through VLM  
 309 input-output interfaces, maintaining compatibility with both  
 310 open-source and commercial models without requiring ac-  
 311 cess to internal representations.

### 312 5. Experimental Evaluation

313 We evaluate PixelSHAP’s effectiveness for object-level  
 314 attribution in vision-language models through systematic  
 315 comparison with existing black-box methods on carefully  
 316 constructed human-annotated datasets.

#### 317 5.1. Dataset Construction

318 The absence of suitable benchmarks for object-level  
 319 VLM attribution necessitated creating specialized evalua-  
 320 tion datasets. We developed two complementary datasets  
 321 with human annotation protocols designed to assess object-  
 322 level interpretability across different visual domains.

323 **BDD10K Traffic Dataset:** We selected 250 rep-  
 324 resentative images from the Berkeley DeepDrive dataset  
 325 (BDD10K) [18], focusing on driving scenarios containing  
 326 multiple traffic participants (vehicles, pedestrians, cyclists,  
 327 traffic signs). Each scene was chosen to represent common  
 328 driving situations where understanding object-level atten-  
 329 tion becomes safety-critical: intersections with multiple ve-  
 330 hicles, crosswalks with pedestrians, and complex urban en-  
 331 vironments with mixed traffic.

332 Three experienced annotators followed a structured pro-  
 333 tocol: first, they randomly selected one object from each  
 334 traffic scene, then formulated driving-relevant questions  
 335 that would require focusing on that specific object to answer  
 336 correctly (e.g., “Which vehicle poses the greatest safety  
 337 concern?” or “What traffic element should influence the  
 338 driver’s next action?”). This approach ensures unbiased  
 339 ground truth while maintaining realistic question formula-  
 340 tion. We measured inter-annotator agreement using Fleiss’  
 341 kappa [2] and retained only scenes achieving substantial  
 342 consensus ( $\kappa > 0.7$ ). Figure 3 illustrates representative ex-  
 343 amples from this dataset, showing the diversity of objects  
 344 and question types used in evaluation.

345 **COCO General Dataset:** To demonstrate broader ap-  
 346 plicability beyond traffic scenarios, we created a comple-  
 347 mentary dataset using 250 images selected from COCO [5]  
 348 validation set. Following identical annotation protocols, an-  
 349notators first randomly selected objects from general visual  
 350 scenes, then generated focused questions requiring attention  
 351 to those specific objects. This dataset enables assessment  
 352 of PixelSHAP’s effectiveness across diverse visual contexts  
 353 while maintaining the same evaluation framework.

354 Both datasets are publicly available on Hugging

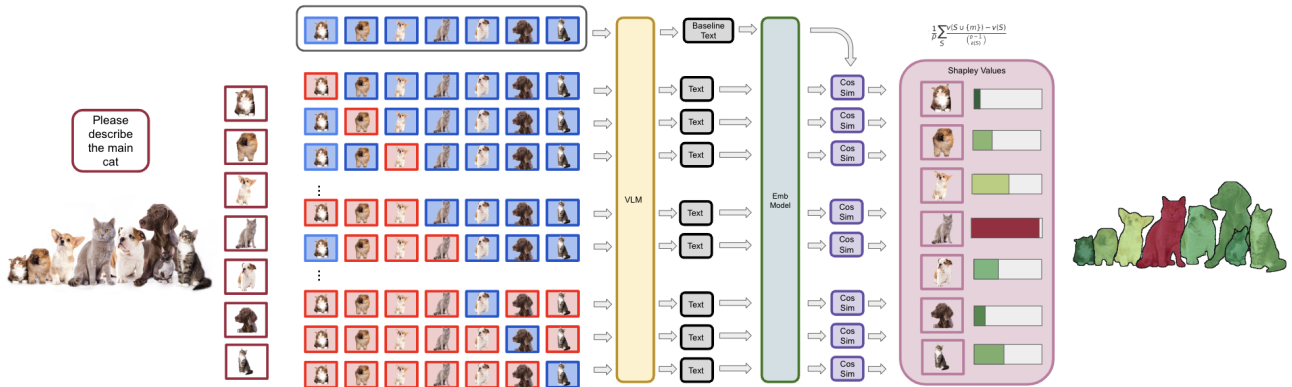


Figure 2. Overview of the PixelSHAP framework. The method systematically perturbs object groups, queries a vision-language model (VLM), and computes Shapley values to quantify object importance.



Figure 3. Sample annotations from BDD10K Traffic Dataset showing diverse object types and corresponding questions. Each example demonstrates how human annotators formulated questions requiring attention to specific objects for accurate answering.

355  
356

Face[17], providing standardized benchmarks for future research in object-level VLM interpretability.

357

## 5.2. Evaluation Protocol

358  
359  
360  
361  
362  
363  
364  
365

Our evaluation protocol measures how well attribution methods identify the same objects that human experts consider most relevant for answering given questions. For each image-question pair, we provide the question and corresponding answer to the VLM, then apply different attribution methods to identify which objects the model should focus on. We compare these attributions against human annotations to assess attribution quality.

366  
367  
368  
369

This framework enables direct comparison of different attribution approaches while maintaining consistency with human reasoning patterns about object relevance in visual question answering tasks.

## 5.3. Masking Strategies

PixelSHAP’s effectiveness depends critically on the masking strategy used during object occlusion. We investigate two primary approaches for handling object removal during attribution computation:

**Precise Masking:** Objects are masked exactly according to their segmentation boundaries, replacing object pixels with neutral background or inpainting [9]. This approach maintains precise object boundaries but may create artificial visual artifacts at object edges.

### Bounding Box Occlusion with Adjustment (BBOA):

Objects are occluded using expanded bounding boxes that fully contain the object while minimizing overlap with neighboring objects. This strategy avoids edge artifacts and prevents unintended masking of adjacent objects that might confound attribution computation.

Figure 4 illustrates these different masking approaches and their impact on attribution quality. The BBOA strategy demonstrates superior performance by ensuring complete object occlusion while preserving the integrity of surrounding visual context.

## 5.4. Baseline Comparison Framework

We establish PixelSHAP’s effectiveness through comparison with existing black-box interpretability methods adapted for object-level analysis. Since direct comparison requires operating at the same semantic granularity, we adapt pixel-level methods to produce object-level attributions.

**Rise-Objects:** The original RISE method [10] generates pixel-level importance maps through random masking. We adapt RISE to operate at object-level granularity by randomly masking subsets of detected objects and measuring resulting changes in model output similarity. This preserves RISE’s core perturbation methodology while enabling fair

370  
371  
372  
373  
374  
375  
376  
377  
378  
379  
380  
381  
382  
383  
384  
385  
386  
387  
388  
389  
390

391  
392  
393  
394  
395  
396  
397  
398  
399  
400  
401  
402  
403

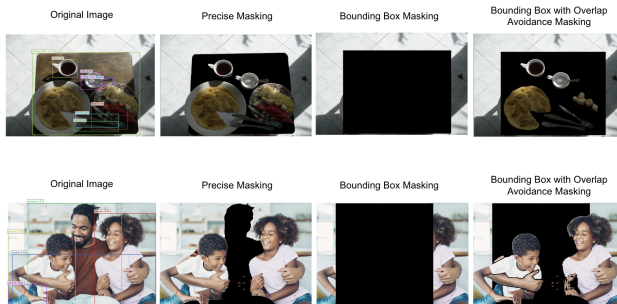


Figure 4. Comparison of masking strategies for object occlusion in PixelSHAP. (a) Precise masking follows exact segmentation boundaries. (b) Bounding Box Occlusion with Adjustment (BBOA) uses expanded boxes to ensure complete occlusion while minimizing interference with neighboring objects. BBOA consistently achieves better attribution performance across different scenarios.

404 comparison at the semantic object level.

405 **Simple Heuristic Baselines:** We include largest object  
406 (by bounding box area) and central object (closest to image center)  
407 as basic attribution methods. These baselines test whether sophisticated attribution approaches provide  
408 meaningful improvements over simple assumptions about visual  
409 attention.

410 **Random Baseline:** Random object selection establishes  
411 the performance floor and validates that our evaluation metrics  
412 capture meaningful attribution quality differences.

## 414 5.5. Evaluation Metrics

415 We assess attribution quality using metrics aligned with  
416 human annotation protocols and practical interpretability  
417 needs:

418 **Recall@1:** Percentage of test cases where the highest-  
419 attributed object matches human expert annotation. This  
420 metric directly measures whether attribution methods iden-  
421 tify the same object that human experts consider most relevant.

422 **Recall@3:** Percentage where the human-annotated target  
423 object appears among the top-3 attributed objects, pro-  
424 viding insight into attribution ranking quality.

425 **Mean Reciprocal Rank (MRR):** Average inverse rank  
426 of the ground-truth object across all test cases, offering a nu-  
427 nanced view of attribution accuracy that accounts for ranking  
428 position.

## 430 5.6. Results and Analysis

431 Table 1 presents comprehensive performance comparison  
432 across four representative VLMs on both datasets. The  
433 results demonstrate that PixelSHAP with BBOA mask-  
434 ing achieves the best performance in nearly all scenarios,

though some competitive cases reveal interesting model-specific characteristics.

**Model-Specific Performance Patterns:** Gemini-2.0-flash achieves the highest overall performance across both datasets, with particularly strong results on COCO general scenes (67.48% Recall@1) and leading performance on traffic scenarios (64.7% Recall@1). GPT-4o demonstrates competitive performance on traffic scenarios (63.8% Recall@1), while both LLaVA-v1.5-7B and LLaMA-3.2-11B-Vision show more modest but consistent results across datasets.

**Masking Strategy Analysis:** BBOA achieves the best performance in the vast majority of cases, though some notable exceptions highlight the complexity of optimal masking strategies. LLaMA-3.2-11B-Vision shows a rare case where precise masking slightly outperforms BBOA on traffic Recall@1 (56.1% vs 55.8%), while LLaVA-v1.5-7B demonstrates competitive performance where precise masking achieves higher Recall@3 and MRR scores on traffic scenarios. These close margins suggest that masking strategy optimization may be model-dependent in specific contexts.

**Attribution Method Robustness:** The consistently strong performance of BBOA across different models and datasets validates our approach, with typical improvements of 3-8 percentage points over precise masking and 10-20 percentage points over baseline methods. The few competitive cases where precise masking approaches BBOA performance (difference 0.3 percentage points) demonstrate that while BBOA is generally superior, the optimal strategy may require fine-tuning for specific model architectures.

**Baseline Comparison:** PixelSHAP variants substantially outperform simple heuristics and RISE-Objects across all conditions. RISE-Objects achieves moderate performance but consistently lags behind PixelSHAP approaches by 5-15 percentage points in Recall@1, confirming the benefits of principled Shapley-based attribution for object-level interpretability.

**Dataset-Specific Insights:** Performance patterns show interesting domain dependencies. Gemini-2.0-flash maintains strong advantages on both datasets, suggesting robust generalization capabilities. The traffic scenarios generally yield slightly higher absolute performance across models, potentially reflecting the more structured nature of driving scenes compared to diverse COCO imagery.

## 480 5.7. Computational Efficiency

PixelSHAP processing requires 35-65 seconds per image depending on object count and VLM inference speed, using approximately 2-3× the number of detected objects in API calls rather than the exponential scaling that naive Shapley computation would require. This represents practical computational requirements suitable for offline analysis and

435

436

437

438

439

440

441

442

443

444

445

446

447

448

449

450

451

452

453

454

455

456

457

458

459

460

461

462

463

464

465

466

467

468

469

470

471

472

473

474

475

476

477

478

479

Model	Method	BDD10K Traffic Dataset			COCO General Dataset		
		R@1 (%)	R@3 (%)	MRR	R@1 (%)	R@3 (%)	MRR
GPT-4o	PixelSHAP (BBOA)	<b>63.8</b>	<b>86.2</b>	<b>0.75</b>	<b>60.56</b>	<b>87.66</b>	<b>0.73</b>
	PixelSHAP (Precise)	59.2	82.1	0.71	57.61	84.71	0.69
	PixelSHAP (BBox)	55.7	78.4	0.67	53.18	85.20	0.68
	RISE-Objects	43.1	67.8	0.57	42.3	69.2	0.56
Gemini-2.0-flash	PixelSHAP (BBOA)	<b>64.7</b>	<b>85.9</b>	<b>0.76</b>	<b>67.48</b>	<b>89.17</b>	<b>0.77</b>
	PixelSHAP (Precise)	62.1	83.2	0.73	59.62	84.73	0.71
	PixelSHAP (BBox)	59.4	80.8	0.71	58.10	88.68	0.72
	RISE-Objects	47.6	72.1	0.61	45.7	71.6	0.59
LLaVA-v1.5-7B	PixelSHAP (BBOA)	<b>48.9</b>	71.4	0.61	<b>49.78</b>	<b>83.28</b>	<b>0.65</b>
	PixelSHAP (Precise)	48.2	<b>72.1</b>	<b>0.62</b>	49.27	75.38	0.61
	PixelSHAP (BBox)	45.6	68.9	0.59	43.88	76.32	0.59
	RISE-Objects	41.3	65.7	0.55	37.2	64.5	0.52
LLaMA-3.2-11B-Vision	PixelSHAP (BBOA)	55.8	<b>78.3</b>	<b>0.68</b>	<b>52.71</b>	<b>86.72</b>	<b>0.68</b>
	PixelSHAP (Precise)	<b>56.1</b>	77.9	0.68	49.76	80.27	0.64
	PixelSHAP (BBox)	53.4	76.2	0.66	50.76	80.32	0.65
	RISE-Objects	44.8	68.5	0.58	38.9	66.4	0.53
<b>Largest Object</b>		38.4	62.5	0.51	23.14	60.85	0.43
<b>Central Object</b>		31.7	58.1	0.46	36.92	70.62	0.52

Table 1. Object-level attribution performance comparison across VLMs and datasets. Results show mean performance over test sets. Bold indicates best performance for each model-method combination.

safety validation applications in autonomous driving systems.

## 487 488 489 5.8. Limitations and Future Work

490 Our evaluation reveals several limitations that inform future  
491 research directions. Performance degrades in extremely  
492 cluttered scenes ( $> 15$  objects) where occlusion becomes  
493 pervasive. Attribution quality also depends on segmenta-  
494 tion accuracy, creating dependency on upstream computer  
495 vision components.

496 **Segmentation Quality Impact:** We evaluate attribution  
497 degradation under noisy segmentation by introducing con-  
498 trolled errors (10-30% mask boundary deviation) to ground-  
499 truth objects. Performance drops 8-15% with moderate  
500 noise, confirming segmentation dependency while demon-  
501 strating reasonable robustness to realistic segmentation er-  
502 rors.

503 The varying performance patterns across models suggest  
504 that future work should explore model-specific attribution  
505 strategies that account for architectural differences in visual  
506 reasoning capabilities.

## 507 5.9. Qualitative Examples

508 Figure 5 demonstrates PixelSHAP’s ability to provide in-  
509 tuitive, context-sensitive attributions across different query  
510 types and scenarios.



Figure 5. PixelSHAP attribution examples across traffic and general scenarios. Each row shows the same scene analyzed with different questions, demonstrating context-sensitive attribution. Red intensity indicates object importance scores.

511 **Traffic Scene Analysis:** In driving scenarios, PixelSHAP  
512 correctly prioritizes safety-critical objects based  
513 on query context. When asked “Which vehicle should  
514 the driver monitor?”, the method emphasizes the approach-  
515 ing car rather than parked vehicles. For pedestrian-  
516 focused queries like “Is it safe to proceed?”, attribution  
517 shifts to highlight the person near the crosswalk while de-  
518 emphasizing background traffic.

519      **Context Sensitivity:** The examples demonstrate sophis-  
520      ticated adaptation to query specificity. Identical visual  
521      scenes produce different attribution patterns when analyzed  
522      with different questions. General queries about scene con-  
523      tent distribute attention across multiple objects, while spe-  
524      cific queries about particular object types concentrate attri-  
525      bution on relevant entities.

526      **General Scene Understanding:** Beyond traffic applica-  
527      tions, PixelSHAP provides meaningful attributions for  
528      diverse visual reasoning tasks. When analyzing animal  
529      scenes, queries about "What animals are present?" appro-  
530      priately emphasize biological entities while ignoring back-  
531      ground objects. Action-focused questions shift attribution  
532      toward objects involved in activities rather than static scene  
533      elements.

534      These qualitative results confirm that PixelSHAP cap-  
535      tures the contextual reasoning that makes VLM inter-  
536      pretability valuable for practical applications. The method's  
537      ability to adapt attribution patterns based on query intent en-  
538      ables users to understand not just what objects are visually  
539      prominent, but which objects actually influence the model's  
540      reasoning for specific tasks.

## 541      6. Discussion

542      Our work fills a critical gap in understanding how Vision-  
543      Language Models (VLMs) reason about traffic scenes, of-  
544      fering practical tools for safety validation in autonomous  
545      driving.

### 546      6.1. Key Findings

547      PixelSHAP extends Shapley-based attribution to object-  
548      level analysis while maintaining black-box compatibility,  
549      essential for commercial VLMs. The BBOA masking strat-  
550      egy resolves the core challenge of occluding target objects  
551      without interfering with surrounding context, outperform-  
552      ing existing perturbation methods.

553      Consistent performance across diverse VLM architec-  
554      tures indicates that our approach captures fundamental as-  
555      pects of vision-language reasoning for traffic under-  
556      standing. While commercial models achieve higher absolute at-  
557      tribution accuracy, relative gains from object-level analysis  
558      remain comparable across architectures.

559      For autonomous driving, PixelSHAP allows engineers to  
560      verify that VLMs attend to the correct traffic participants,  
561      supporting validation workflows critical for safe deploy-  
562      ment.

### 563      6.2. Limitations

564      Attribution accuracy depends on segmentation quality,  
565      making it reliant on upstream detection performance. Cur-  
566      rent processing times (35–65 seconds per image) suit offline  
567      analysis but limit real-time use.

568      Though BBOA minimizes distribution shift, masking  
569      can still alter image statistics, especially in cluttered scenes  
570      with over 15 objects. Evaluation relies on human annota-  
571      tions, which may not fully capture expert safety priorities.

## 572      6.3. Future Directions

573      **Integration with Autonomous Systems:** Embedding attri-  
574      bution into development workflows could enable continu-  
575      ous validation during system updates. **Temporal Analy-**  
576      **sis:** Extending to video sequences would support reason-  
577      ing about dynamic object importance. **Domain-Specific**  
578      **Models:** Adapting the framework for traffic-specific cate-  
579      gories (e.g., emergency vehicles, construction zones) could  
580      improve safety-critical assessments. **Computational Op-**  
581      **timization:** Approximation models may accelerate attribu-  
582      tion, enabling iterative development workflows.

## 583      7. Conclusion

584      We introduced PixelSHAP, a model-agnostic framework for  
585      object-level attribution in Vision-Language Models for traf-  
586      fic scene understanding. By extending Shapley value attri-  
587      bution to structured visual entities, our approach provides  
588      meaningful explanations that enable safety validation in au-  
589      tonomous driving.

590      Through systematic evaluation, we demonstrated consist-  
591      ent improvements over prior methods. Our BBOA mask-  
592      ing strategy addresses key challenges in perturbation-based  
593      attribution while supporting compatibility with commercial  
594      VLMs.

595      PixelSHAP empowers engineers to identify which traf-  
596      fic participants influence model decisions, supporting safety  
597      validation workflows for autonomous systems. Our open-  
598      source implementation facilitates adoption in research and  
599      practice. Future work should focus on computational ef-  
600      ficiency and integration into autonomous vehicle develop-  
601      ment pipelines to enhance transportation safety.

## 602      Supplementary Material

603      Additional materials including code, datasets, and extended  
604      results will be made available upon acceptance to maintain  
605      anonymity during the review process.

## 606      References

- [1] Google DeepMind. Gemini 2.0 pro, 2024. Released as part of Gemini AI Suite. [2](#)
- [2] Joseph L. Fleiss. Measuring nominal scale agreement among many raters. *Psychological Bulletin*, 76(5):378–382, 1971. [4](#)
- [3] Miriam Horovitz and Roni Goldshmidt. Tokenshap: Interpreting large language models with monte carlo shapley value estimation. In *EMNLP NLP4Science Workshop*, 2024. [2](#)

- 615 [4] Alexander Kirillov, Eric Mintun, Nikhila Ravi, Hanzi Mao,  
616 Yuxin Rolland, Linus Gustafson, Trevor Xiao, Spencer  
617 Whitehead, Alexander C. Berg, Wan-Yen Lo, Piotr Dollár,  
618 and Ross Girshick. Segment anything. *arXiv preprint*, 2023.  
619 4
- 620 [5] Tsung-Yi Lin, Michael Maire, Serge Belongie, Lubomir D.  
621 Bourdev, Ross B. Girshick, James Hays, Pietro Perona,  
622 Deva Ramanan, Piotr Dollár, and C. Lawrence Zitnick. Mi-  
623 crosoft coco: Common objects in context. *arXiv preprint*,  
624 abs/1405.0312, 2014. 4
- 625 [6] Shilong Liu, Feng Li, Hao Zhang, Xiao Zhang, Lei Zhu,  
626 Hang Wang, Jianlong Shi, Hongyang Li, and Hao Dong.  
627 Grounding dino: Marrying dino with grounded pre-training  
628 for open-set object detection. *arXiv preprint*, 2023. 4
- 629 [7] OpenAI. Gpt-4o model card, 2024. Accessed via OpenAI  
630 API. 2
- 631 [8] L. Parcalabescu and A. Frank. Mm-shap: Multimodal shap-  
632 ley values for model interpretation. *arXiv preprint*, 2022. 2
- 633 [9] Deepak Pathak, Philipp Krahenbuhl, Jeff Donahue, Trevor  
634 Darrell, and Alexei A. Efros. Context encoders: Feature  
635 learning by inpainting. In *IEEE Conf. Comput. Vis. Pattern  
636 Recog.*, pages 2536–2544, 2016. 5
- 637 [10] V. Petsiuk, A. Das, and K. Saenko. Rise: Randomized input  
638 sampling for explanation of black-box models. In *British  
639 Machine Vision Conference (BMVC)*, 2018. 2, 5
- 640 [11] Joseph Redmon, Santosh Divvala, Ross Girshick, and Ali  
641 Farhadi. You only look once: Unified, real-time object de-  
642 tection. In *IEEE Conference on Computer Vision and Pattern  
643 Recognition (CVPR)*, pages 779–788, 2016. 4
- 644 [12] Nils Reimers and Iryna Gurevych. Sentence-bert: Sentence  
645 embeddings using siamese bert-networks. In *Proceedings of  
646 the 2019 Conference on Empirical Methods in Natural Lan-  
647 guage Processing and the 9th International Joint Conference  
648 on Natural Language Processing (EMNLP-IJCNLP)*, pages  
649 3982–3992, 2019. 4
- 650 [13] Marco Tulio Ribeiro, Sameer Singh, and Carlos Guestrin.  
651 Why should i trust you? explaining the predictions of any  
652 classifier. In *Proceedings of the ACM SIGKDD Interna-  
653 tional Conference on Knowledge Discovery and Data Min-  
654 ing (KDD)*, page 1135–1144, 2016. 2
- 655 [14] Ramprasaath R. Selvaraju, Michael Cogswell, Abhishek  
656 Das, Ramakrishna Vedantam, Devi Parikh, and Dhruv Ba-  
657 tra. Grad-cam: Visual explanations from deep networks via  
658 gradient-based localization. In *Int. Conf. Comput. Vis.*, pages  
659 618–626, 2017. 2
- 660 [15] Lloyd S. Shapley. A value for n-person games. *Contributions  
661 to the Theory of Games*, 2:307–317, 1953. 2
- 662 [16] G. B. M. Stan, R. Saunshi, N. Viswanathan, G. Sun-  
663 daramoorthi, and A. Menon. Lvlm-interpret: An inter-  
664 pretability tool for large vision-language models. In *CVPR  
665 Workshop on Explainable AI for Computer Vision*, 2024. 2
- 666 [17] Thomas Wolf, Lysandre Debut, Victor Sanh, Julien Chau-  
667 mond, Clement Delangue, Anthony Moi, Perric Cistac, Tim  
668 Rault, Rémi Louf, Morgan Funtowicz, Joe Davison, Sam  
669 Shleifer, Patrick von Platen, Clara Ma, Yacine Jernite, Julien  
670 Plu, Canwen Xu, Teven Le Scao, Sylvain Gugger, Mariama  
671 Drame, Quentin Lhoest, and Alexander M. Rush. Trans-  
672 formers: State-of-the-art natural language processing. In
- 673 *Proceedings of the 2020 Conference on Empirical Methods  
in Natural Language Processing: System Demonstrations*,  
674 pages 38–45, 2020. 5
- 675 [18] Fisher Yu, Haofeng Chen, Xin Wang, Wenqi Xian, Yingying  
676 Chen, Fangchen Liu, Vashisht Madhavan, and Trevor Dar-  
677 rell. Bdd100k: A diverse driving dataset for heterogeneous  
678 multitask learning. In *The IEEE Conference on Computer  
679 Vision and Pattern Recognition (CVPR)*, 2020. 4
- 680